Optics and Laser Technology 108 (2018) 609–618

Contents lists available at ScienceDirect

Optics and Laser Technology

journal homepage: www.elsevier.com/locate/optlastec

Full length article

Influence of Dy doping on key linear, nonlinear and optical limiting characteristics of SnO_2 films for optoelectronic and laser applications

Mohd. Shkir [a], Mohd Taukeer Khan [b], V. Ganesh [a], I.S. Yahia [a], Bakhtiar Ul Haq [a], Abdullah Almohammedi [b], Parutagouda Shankaragouda Patil [c], Shivaraj R. Maidur [c], S. AlFaify [a,*]

[a] Advanced Functional Materials and Optoelectronics Laboratory (AFMOL), Department of Physics, College of Science, King Khalid University, Abha 61413, P.O. Box 9004, Saudi Arabia
[b] Department of Physics, Faculty of Science, Islamic University of Madinah, Madinah, Saudi Arabia
[c] Department of Physics, K.L.E. Institute of Technology, Opposite Airport, Gokul, Hubballi 580030, India

ARTICLE INFO

Article history:
Received 2 March 2018
Accepted 16 July 2018

Keywords:
Thin films
XRD
Raman spectroscopy
SEM/EDX
Optical properties
Non-linear optical properties

ABSTRACT

In the present work, pure and dysprosium (Dy) doped SnO_2 films have been fabricated through sol-gel spin coating technique. Strong influence of Dy doping is observed on structural, morphological, vibrational, linear and nonlinear optical properties of SnO_2 films. X-ray diffraction study revealed that deposited films exhibit tetragonal crystal structure with preferentially grown along (2 0 0) plane. With increase of doping concentration in SnO_2, the crystallite size decreases while dislocation density and lattice distortion ratio increases. The characteristics Raman peaks of doped SnO_2 thin films broaden, shifted and intensity decreases as compared to pure film which confirm the bonding between Dy and SnO_2. Optical study shows that the prepared thin films are highly transparent and absorption increases with doping concentrations owing to increase of defects states. It is also observed that the optical band gap first increases and then lessens with rise of Dy-doping concentration which attributed to the Burstein-Moss (BM) effect. Additionally, dielectric constant and refractive index first decreasing with small doping concentration (1–3%) due to increase of carrier concentration, and then increases for higher doping (5–7%) due to increase of defect in SnO_2 lattice. The values $\chi^{(3)}$ and β obtained by Z-scan measurement are observed in range of 0.31×10^{-7} to 1.28×10^{-7} and 1.27 to 5.32×10^{-4} cm W^{-1}, respectively. The limiting threshold of pure and Dy doped SnO_2 nanostructured films were calculated to be in the range of 5.37–11.18 kJ/cm^2.

1. Introduction

Tin oxide (SnO2) thin films can be easily prepared by environmentally safe, non-toxicity and cost-effective methods. In recent years, tin oxide (SnO_2) has attracted extensive attention for its potential applications in optoelectronic devices like: LED [1], solar cells [2], transistors [3], and gas sensors [4]. The main attractive aspect of SnO_2 is its unique nature of low resistivity and high transmittance in the visible region [5–7]. Moreover, it have wide band-gap in the range of 3.6–4.1 eV [8] and very high exciton binding energy of 130 meV [9] at room temperature which enable us to observe the exciton related phenomena at room temperature [10], not possible in other metal oxide thin films.

Tin oxide films are reported to be readied by various techniques like: pulsed laser deposition, reactive magnetron sputtering, atomic layer deposition, chemical vapor deposition, microwave-assisted methods, electron beam evaporation, hydrothermal deposition, sputtering, dip coating, spray pyrolysis, vapor-liquid-solid synthesis, thermal evaporation method, and sol-gel methods [11–19]. Among these techniques for thin film preparation, sol-gel spin coating method is one of the most promising method due to simplicity of deposition, low cost of the used materials and equipment. With this technique, wider film areas can be produced and enables to control the key characteristics of thin films according to device requirement.

Herein, we fabricate thin films of SnO_2 as pure and in presence of Dy dopant by spin coating method due to compatibility of this method with the future optoelectronic devices which are prepared by low cost solution method.

In recent years, the rare earth elements (e.g. Dy, Ce, Gd, La, , Nd, Sm,. . .. . .) doped nanoparticles have shown improved luminescence, photocatalyst and electrical properties. Dysprosium, Dy, is an emissive dopant and optical properties of it depends on f-f

* Corresponding author.
E-mail address: sasaalfaify@hotmail.com (S. AlFaify).

https://doi.org/10.1016/j.optlastec.2018.07.039
0030-3992/

transition electrons. These electrons are localized to atomic orbitals and do not shows quantum confinement effect. However, it is expected that the photogenerated carrier created from confinement effect of SnO_2 nanoparticle, may interact with f-electrons and change the optical properties of SnO_2 or show completely new properties.

Previously, very few works have been reported on SnO_2 films doped with Dy. In earlier studies, the main focus was on structural, luminescence chattels of Dy- doped SnO_2. Joseph et al. have prepared thin films of SnO_2 by vapor deposition method and studied the Dy-doping consequences on several chattels [15]. Pillai et al. have prepared films of SnO_2 with Dy doping by chemical co-precipitation methods and analyze their structural and luminescence properties [20]. Feng et al. have synthesized the Dy^{+3} dope SnO2 nanoparticles by a sol–gel method and samples were investigated for structural and luminescence properties [21]. However, still some experimental studies related to linear and nonlinear optical parameters such as refractive index, susceptibility, dielectric constant etc. are absent.

The main objective of this work is to elucidate the influence on linear, non-linear optical and optical limiting characteristics of SnO_2 films through Dy-doping readied by spin coating. The prepared films have been investigated spectroscopically by using XRD, SEM, Raman and UV–Vis absorption spectra. Various linear and non-linear optical parameters such as optical band gap, dielectric constant, refractive index, susceptibility etc. have also been extracted from these results. Z-scan study was also performed.

2. Materials and methods/experimental

For fabricating the films of pure and Dy doped SnO_2 on glass substrates the following materials are used: $SnCl_2.5H_2O$ as precursor, ethylene glycol, isopropyl alcohol solvents and $Dy(NO_3)_3{\cdot}xH_2O$ as dopant were bought from Sigma Aldrich Pvt. ltd. Cleaning of substrate, preparation of gel and thin films fabrication process by spin coating, heating, annealing of films and their characterization techniques are similar to our previous report including Z-scan [26,27]. Thicknesses of films were found in range of 150 to 300 nm.

3. Results and discussions

3.1. Structural analysis

The structural analysis of all films was investigated by XRD study in 2θ range 35–70°. The X-ray diffraction pattern of these films are shown in Fig. 1 and the corresponding calculated lattice parameters are given in Table 1. It is observed from the Fig. 1 that the films have poly crystalline structure. Peak at 38.2° corresponds to the (2 0 0) plane while at 42.5° corresponds to the (2 1 0) plane in accordance to the JCPDS data card no 41-1445 [22]. The lattice constants for the prepared films have been calculated by using Eq. (1) [23]:

$$\frac{1}{d^2}=\frac{h^2}{a^2}+\frac{k^2}{b^2}+\frac{l^2}{c^2} \tag{1}$$

The calculated lattice constants for pure SnO_2 thin films are a = b = 4.738 Å and c = 3.187 Å, which are well agreed with earlier report [22]. In Fig. 1, no additional characteristics peaks of dopant (such as dysprosium oxide or other tin oxides phases) were detected. This indicates that the structure of SnO_2 thin films is not affected by Dy doping. Further effects of Dy on SnO_2 structure were analyzed by evaluating dislocation density, crystallite size, number of unit cells, and lattice distortion ratio.

Debye-Scherer formula were used to calculate the average crystallite size D of these films [24–26]:

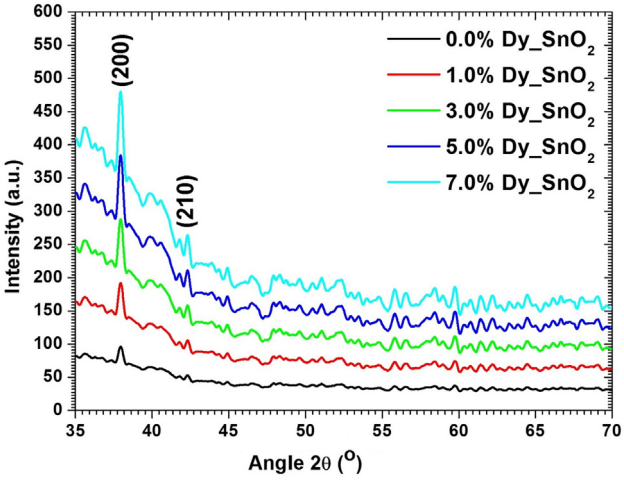

Fig. 1. X-ray diffraction patterns of all fabricated films.

$$D=\frac{0.9\lambda}{\beta_{hkl}\cos\theta} \tag{2}$$

where θ is angle, λ is wavelength, and β_{hkl} is FWHM. Crystalline sizes for pure and Dy-doped SnO_2 films calculated by Eq. (2) are given in Table 1. It is visible from Table 1 that crystallite size decreases with Dy concentrations in SnO_2 thin films. The size of Dy ion is bigger than Sn, subsequently, Dy-doping triggered pressure built in crystal lattice which hinder the crystal growth [28]. The lattice strain, ε of prepared films was calculated from the Eq. [28,29]:

$$\varepsilon=\frac{\beta\cos\theta}{4} \tag{3}$$

It is visible from table that the lattice distortion ratio increased with increase of Dy-doping in SnO_2 thin films. Increase in distortion ratio on doped films, increase the number of defects [30], as a result, deterioration of the crystalline quality. This outcome could be justified by further evaluating the number of unit cells (n) and dislocation density (δ) of prepared thin films from Eqs. (4) and (5), respectively [29,31]:

$$n=\frac{\pi D^3}{6V} \tag{4}$$

$$\delta=\frac{1}{D^2} \tag{5}$$

Dislocation density gives the information about the quality of film and defects present in the material [32,33]. The calculated number of unit cells and dislocation density are presented in Table 1. From tabulated data it is evident that the number of unit cells decreases and dislocation density increases with increase of dopant concentration which again confirm the deterioration of the film quality.

3.2. FT-Raman spectroscopy analysis

FT-Raman spectra were measured to confirm the Dy-doping and consequential changes in vibrational modes of SnO_2 thin films. Unit cell of SnO_2 lattice having four oxygen and two tin atoms. These 6 atoms provide 18 normal vibrational modes in the first Brillouin zone and given by [34–37]:

$$\Gamma=\Gamma_1^+(A_{1g})+\Gamma_2^+(A_{2g})+\Gamma_3^+(B_{1g})+\Gamma_4^+(B_{2g})+\Gamma_5^-(E_g)+2\Gamma_1^-(A_{2u})+2\Gamma_4^-(B_{1u})+4\Gamma_5^+(E_u) \tag{6}$$